Journal of Solid State Chemistry 182 (2009) 2530–2534

Contents lists available at ScienceDirect

Journal of Solid State Chemistry

journal homepage: www.elsevier.com/locate/jssc

Synthesis of sulfated titania supported on mesoporous silica using direct impregnation and its application in esterification of acetic acid and *n*-butanol

Yuhong Wang [a,*], Yunting Gan [a], Roger Whiting [b], Guanzhong Lu [a]

[a] Research Institute of Applied Catalysis, School of Chemical and Environmental Engineering, Shanghai Institute of Technology, Shanghai 200235, Peoples Republic of China
[b] School of Applied Science, Faculty of Health and Environmental Sciences, Auckland University of Technology, Auckland, New Zealand

ARTICLE INFO

Article history:
Received 14 April 2009
Received in revised form
24 June 2009
Accepted 4 July 2009
Available online 10 July 2009

Keywords:
Direct impregnation
Sulfated titania
Mesoporous silica
Esterification

ABSTRACT

A new method has been developed for the preparation of sulfated titania (S-TiO_2) supported on mesoporous silica. The use of direct exchange of metal containing precursors for the surfactants in the as-synthesized MCM-41 substrate produced a product with high sulfur content without serious blockage of the pore structure of MCM-41. The pore sizes and volumes of the resultant S-TiO_2/MCM-41 composites were found to vary markedly with the loading of TiO_2. The strong acidic character of the composites obtained was examined by using them as catalysts for the esterification of acetic acid and *n*-butanol.

1. Introduction

Recently much attention has been paid to sulfated titania (S-TiO_2) as a superacid due to its significant catalytic activity in many reactions, such as esterification, isomerization, alkylation, acylation and etherification [1–6]. It has been shown that the catalytic activity of sulfated titania is largely due to its acid properties. Some authors have reported that the catalyst contains both Brönsted and Lewis acid sites which are responsible for this activity [1,3]. Corma et al. [7] reported that, in the case of ZrO_2, higher surface area of the original material gave higher acid strength after sulfation. This finding suggests that the strong acid sites are associated with sites of low coordination such as defects, corners or edges which are more common on the surface of small particles. It is, however, difficult to increase the surface area of titania through conventional preparative methods. Therefore, the relatively small surface area of S-TiO_2 may limit its usefulness as a catalyst.

Mesoporous molecular sieves have potential applications as catalysts for reactions of large molecules due to their large surface area (~1000 m^2/g) [8,9]. However, their acid strength is low due to the amorphous nature of the pore walls which may greatly limit their use [10,11].

A composite material, which can combine the advantages of mesoporous molecular sieves and S-TiO_2, should greatly expand the catalytic capabilities of the material, especially in applications as a strong acid catalyst for reactions containing bulky molecules. However, there have been few reports of a bifunctional catalyst being prepared from sulphated titania on a support of MCM-41. Usually, it has been difficult to maintain the crystalline structure of MCM-41 in strongly acidic media such as the aqueous solutions of titanium sulfate used in the traditional methods for producing catalysts, for example, "two-step" impregnation methods [12], chemical liquid deposition [13], one-step incipient wetness impregnation method [14], etc. It has also proved been difficult to obtain S-TiO_2/MCM-41 with high TiO_2 content.

In this work, a new approach is taken to impregnate a catalyst on the surface of a mesoporous material. Instead of impregnating titanium sulfate onto a calcined porous MCM-41 material, here it was impregnated onto an as-synthesized surfactant/silicate composite. The ion exchange process is efficient enough to induce a large amount of impregnation while the mesostructure is intact. Then a solid-state dispersion method was used to disperse the titania. With this technique, the problem of the pores filling up can be avoided because the surfactant is still almost fill the channels during impregnation–dispersion process.

In the present work, we report a new method of impregnating titanium sulfate onto an as-synthesized surfactant–silicate composite. The effect of using a solid-state dispersion method to prepare S-TiO_2/MCM-41 composites is examined. The catalytic activities of the resultant S-TiO_2/MCM-41 composites were studied by carrying out acetic acid and *n*-butanol esterification reaction. The materials were characterized with XRD, TGA, NH_3-TPD, BET, DRIFT and elemental analysis.

* Corresponding author. Fax: +86 21 6494 5006.
E-mail address: yuhong_wang502@sit.edu.cn (Y. Wang).

0022-4596/$ - see front matter © 2009 Elsevier Inc. All rights reserved.
doi:10.1016/j.jssc.2009.07.003

2. Experimental

2.1. Preparation of S-TiO_2/MCM-41

The S-TiO_2/MCM-41 composites were prepared by direct impregnation of the as-synthesized MCM-41 with the desired amounts of titanium sulfate solution using the following method [15]. Cetyltrimethylammonium bromide (CTAB) was dissolved in distilled water with NaOH ($2\,mol\,L^{-1}$) solution and titanium sulfate solution. Once fully dissolved, the silica source, tetraethoxysilane (TEOS), was added dropwise to the mixture with vigorous stirring at room temperature. The mole composition of the gel mixture was CTAB:TEOS:NaOH:H_2O = 1.0:3.75:1.64:434, and the TiO_2 contents were taken to be 80%, 70%, 60%, 50% and 40%. The pH of the mixture was maintained at 10.2 with 30% ammonia. After heating at 100 °C for 2 days, the product was filtered, washed, dried at 80 °C overnight then calcined at 550 °C for 5 h.

2.2. Characterization

The powder X-ray diffraction (XRD) patterns were recorded on a Rigaku Miniflex diffractometer with CuKα radiation at 40 kV and 45 mA. The surface area and pore size distribution of the supports were measured by nitrogen adsorption–desorption method (ASAP 2020, Micrometitics). The Thermal Gravimetric Analysis (TGA) data were obtained with an SDT Q-600 TG analyzer. The sulfur contents in the calcined samples were determined from VG Elemental/PQ2-Turbo.

Diffuse Reflectance Infrared Fourier Transform (DRIFT) spectra of the S-TiO_2/MCM-41 sample after adsorbing pyridine were recorded. DRIFT spectra of the samples were recorded using a BOMEM MB155 FT-IR/Ramam spectrometer. The sample was pre-heated at 300 °C for 3 h under 10^{-6} mbar vacuum before pyridine vapor was introduced for 30 min. Spectra were acquired from room temperature to 500 °C.

The acidic properties of the samples were determined by TPD (temperature programmed desorption) of chemisorbed ammonia. A 0.2 g sample was placed in the reactor and pretreated in a helium flow, heated to 600 °C at the rate of 10 °C/min, and remained at 600 °C for 2 h. The samples were cooled to 50 °C and an ammonia pulse was injected. After physically absorbed ammonia was purged with helium, TPD was carried out.

2.3. Acetic acid and n-butanol esterification

Acetic acid and *n*-butanol esterification was carried out at 120 °C in a fixed-bed continuous flow reactor operated at atmospheric pressure. Approximately 1.0 g of the catalyst was loaded into the reactor. The liquid acetic acid and *n*-butanol mixture (1:1.1 v/v) was passed over the catalyst at a flow rate of 0.035 mL/min. The steady state was achieved after 2 h of run time. Reaction products were analyzed by using a gas chromatograph (GC-122) equipped with TCD.

3. Results and discussion

3.1. X-ray diffraction

The XRD profiles of the composites of S-TiO_2/MCM-41 with different TiO_2 contents are shown in Fig. 1. It can be seen that MCM-41 exhibits three clear diffraction peaks with lattice spacing of $d = 3.1(hkl = 100)$, $1.9(hkl = 200)$ and $1.7(hkl = 210)$ nm indicating long range hexagonal order of MCM-41. The 2θ values

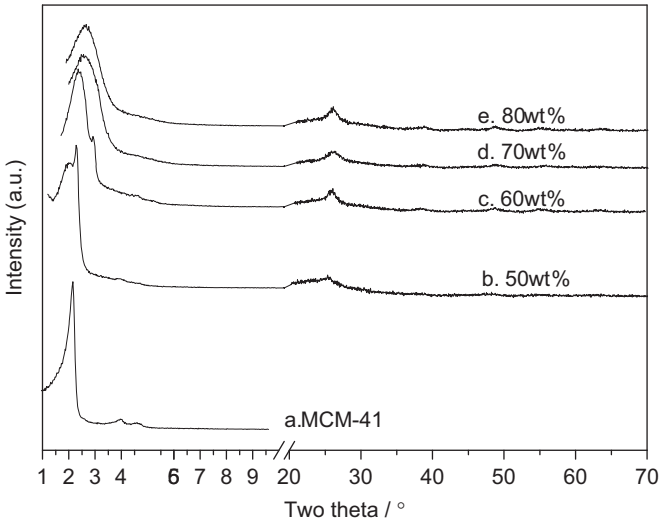

Fig. 1. XRD patterns of the composites of S-TiO_2/MCM-41 with different TiO_2 contents calcined at 550 °C for 5 h in air.

of the d_{100} peaks of the S-TiO_2/MCM-41 samples are extremely similar. This phenomenon indicates that the mesoporous architecture of the MCM-41 is structurally unchanged after modification. In other words, the pore structure of MCM-41 was not destroyed during the solid dispersion processes. However, a gradual loss of long range ordering is observed with increasing TiO_2 loading. This is probably due to an increasing number of defect sites and bond strain in these materials, as evidenced by the decreasing intensities of the [100] peak as well as the higher angle peaks. Also apparent in Fig. 1 are small peaks in the high angle region corresponding to a TiO_2 phase. These peaks appeared when the samples were heated at 550 °C for 5 h. This suggests that the compound of sulfated titania has been decomposed to give SO_x and TiO_2 compounds. Another interesting feature apparent in Fig. 1 is the broadening of prominent d_{100} reflection and shifting higher of the 2θ values with the increased TiO_2 loading. It may be inferred that most of the SO_x and TiO_2 compounds are incorporated into the framework position and/or walls of silica network of MCM-41 [16]. Finally, at relatively high TiO_2 loading, an amorphous material is obtained.

3.2. Physico-chemical properties of the samples

The porosity of the S-TiO_2/MCM-41 samples was evaluated by N_2 adsorption isotherms. Figs. 2 and 3 show the N_2 adsorption–desorption isotherms and the corresponding pore size distribution curves for the S-TiO_2/MCM-41 samples, respectively. Table 1 shows sulfur content, BET surface area, pore diameter and total pore volume of a series S-TiO_2/MCM-41 samples calcined at 550 °C.

As presented in Fig. 2, all the samples showed isotherms of type IV having inflection around $P/P_0 = 0.25$–0.45, characteristic of MCM-41 type ordered mesoporous materials. The samples exhibit complementary textural- and framework-confined mesoporosity, as evidenced by the presence of two separate, well-expressed hysterisis loops. The position of the inflection in the $P/P_0 = 0.25$–0.45 region depends on the diameter of the mesopores and its sharpness indicates the uniformity of the narrow pore size distribution. It can also be seen in Fig. 2 that the point of inflection shifts toward lower relative pressure (P/P_0) with an increase in the TiO_2 content of the S-TiO_2/MCM-41 samples. This indicates a decrease in the pore size. Moreover, the adsorption curve of S-TiO_2/MCM-41 samples changed to a curve similar to

microporous materials, which suggests the incorporation of SO_x and TiO_2 compounds.

It can also be noted from Fig. 2 that the amount of adsorption by sample b (wt% $TiO_2 = 50\%$) increased more sharply in the $P/P_0 = 0.3–0.45$ region than did the amount of adsorption by sample c (wt% $TiO_2 = 70\%$) in the $P/P_0 = 0.25–0.4$ region. This suggests that the pore size of sample b is bigger than that of the sample c as the relative pressure P/P_0 of sample b is higher than the sample c. In other words, the average pore diameters

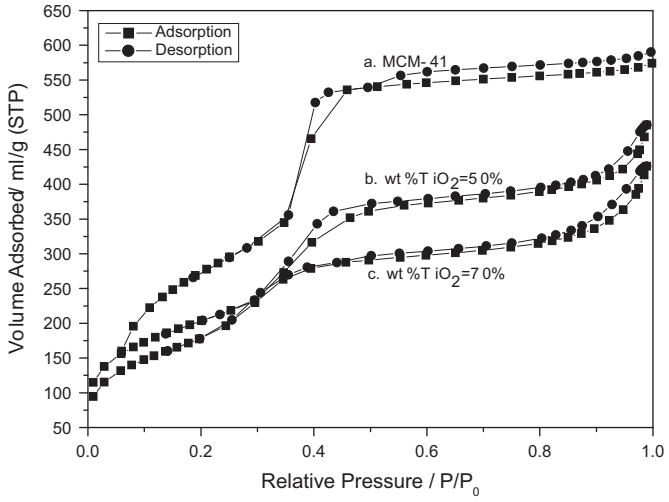

Fig. 2. N_2 adsorption–desorption isotherm of various S-TiO_2/MCM-41 samples.

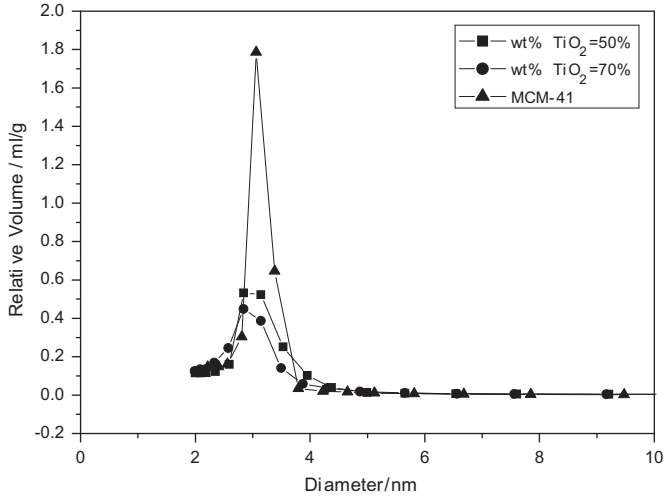

Fig. 3. The pore size distribution curves of MCM-41 and various S-TiO_2/MCM-41 samples.

show a decreasing trend with increasing TiO_2 content of the S-TiO_2/MCM-41 samples. It may be inferred that the decrease in pore size with increasing $Ti(SO_4)_2$ incorporation is due to deposition of SO_x and TiO_2 compounds on the pore surface of cylindrical channels of MCM-41.

From Fig. 3, the pore diameter was also found to decrease gradually with the increase in titania loading. The pore diameter reduced from about 3.1 nm for the parent MCM-41 to about 2.9 nm for the sample b (50 wt% TiO_2), and to 2.8 nm for sample c (70 wt% TiO_2). It is also noticeable that the pore size distributions remain rather narrow for the S-TiO_2/MCM-41 samples. These results confirm that the S-TiO_2 is highly dispersed onto the interior surfaces of the mesopores of MCM-41.

It can be seen from Table 1 that the sulfur content increased with the titania (TiO_2) loading. In contrast, both the BET surface area and pore volume of the samples decreased as the TiO_2 loading increased. The decrease in surface area for the S-TiO_2/MCM-41 samples is attributable to the loss in long-range ordering which is also seen in the XRD pattern. The pore volume decreased due to the deposition of the SO_x and TiO_2 from the decomposition of $Ti(SO_4)_2$.

The uniform decrease of pore size, volume and surface area is an indication that most of the loading of SO_x and TiO_2 is inside the pores. However, at loadings higher than 50%, the decrease in pore volume becomes less marked and the sulfur content increases markedly as shown in Table 1. The 50% TiO_2 content on MCM-41 coincides with the dispersion threshold of titanium sulfate on MCM-41 [17]. This suggests that further loading results in formation of SO_x and TiO_2 particles on the external surface of MCM-41.

3.3. Acidity of S-TiO_2/MCM-41

The acidity of the S-TiO_2/MCM-41 catalyst with 80% TiO_2 loading was monitored by FT-IR using pyridine as a probe molecule (see Fig. 4). The peaks at 1450 cm^{-1} in the spectra are attributed to adsorbed pyridine bound coordinatively to Lewis acid sites. The spectra showed the additional absorption bands at 1540 cm^{-1} which correspond to pyridine interacting with Brönsted acid sites [18]. From the DRIFT spectra (Fig. 4), it can be seen that the intensity of the 1450 and 1540 cm^{-1} peaks slightly decrease as the desorption temperature increases from 200 to 500 °C. However, these two peaks are still apparent even when the sample is held at 500 °C. This implies that the strengths of the Lewis acid sites and Brönsted acid sites on S-TiO_2/MCM-41 catalyst are relatively strong.

The acidic properties of parent $Ti(SO_4)_2$ and the series of S-TiO_2/MCM-41 samples were investigated by ammonia TPD. The profiles of ammonia TPD of samples are shown in Fig. 5. It is obvious that the acidity of S-TiO_2/MCM-41 samples increased with increasing of TiO_2 content, however, their acidity was significantly less than that of parent $Ti(SO_4)_2$ even when the amount of TiO_2 was as high as 80 wt%. As can be seen in

Table 1
Physico-chemical properties of the samples.

wt% TiO_2 in S-TiO_2/MCM-41	Sulfur content (wt%)	BET S.A. (m^2/g)	Pore volume (mL/g)	Esterification rate (%)[a]
40	1.72	763	1.20	22.47
50	2.93	720	0.91	39.44
60	3.94	668	0.81	51.05
70	5.06	631	0.74	77.34
80	9.16	589	0.65	87.62
$Ti(SO_4)_2$	19.77	–	–	90.22

[a] Reaction conditions: temperature—120 °C, acetic acid—10 mL, *n*-butanol—11 mL, catalyst—1 g, and reaction time—2 h.

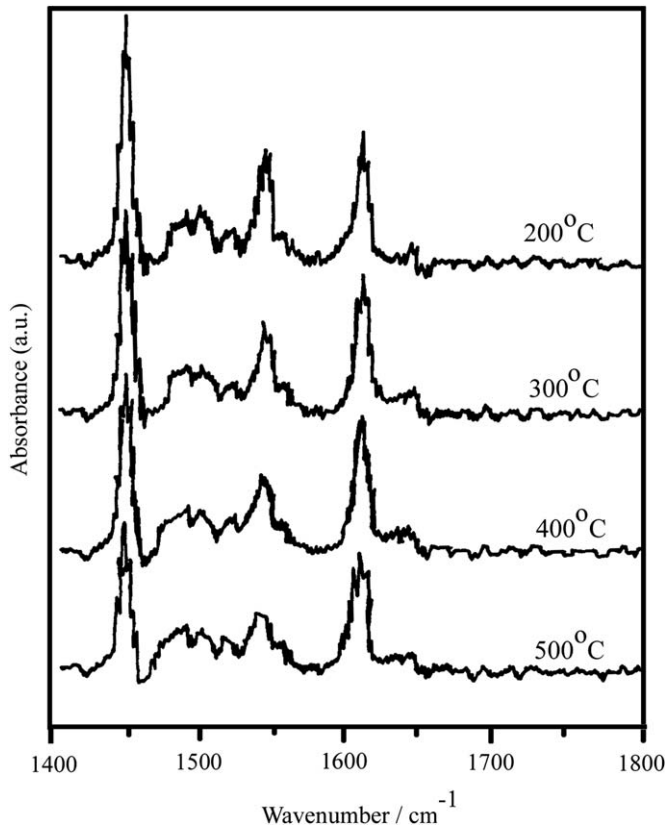

Fig. 4. DRIFT spectra of S-TiO_2/MCM-41 (80 wt% TiO_2) after adsorption of pyridine and evacuation at different temperatures.

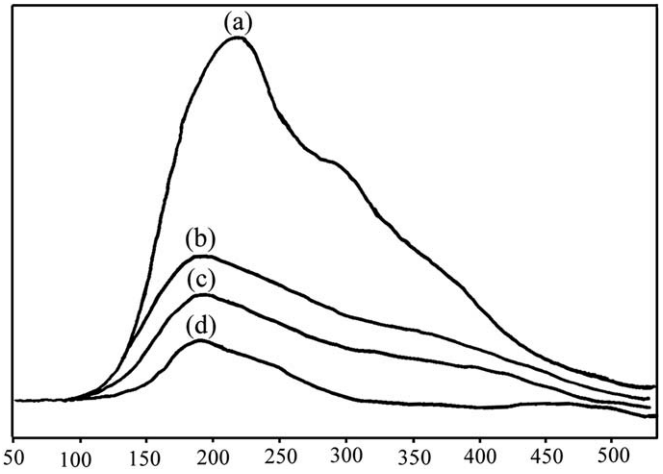

Fig. 5. NH_3-TPD spectra of (a) $Ti(SO_4)_2$ and (b)–(d) S-TiO_2/MCM-41, (b) 80 wt% TiO_2, (c) 70 wt% TiO_2 and (d) 60 wt% TiO_2.

Fig. 5(b)–(d), all of the S-TiO_2/MCM-41 samples show a broad desorption signal in the region 100–400 °C, indicating absorption sites with a wide distribution of the surface acid strengths. Although there is an increase in the concentration of acid sites, Fig. 5(b)–(d) shows an unchanged value in TPD peak maximum. These results are indicative of an overall increase only in the acid site concentration, but NOT in the strength of these sites as a result of the increase in TiO_2 content.

The acidity study also indicates that $Ti(SO_4)_2$ is responsible for the formation of Lewis acid sites and Brönsted acid sites since MCM-41 almost shows no acid properties [10]. It can be concluded that acid sites are bonded with the sulfate species, and their concentration increases with the increase of sulfur content, as shown in Table 1.

3.4. Thermal decomposition analysis

The crystalline structure and surface area of MCM-41 are well retained when as-synthesized MCM-41 rather than a calcined sample is used as starting material for preparation of impregnated catalysts. This is because the space-filling template inside the pores would prevent the complete fill-up of the pore volume with the impregnated precursor [17]. Therefore, in the current preparation method, as-synthesized MCM-41 was used instead of the calcined. TG analysis was carried out to determine the proper temperatures for sample preparation.

The TGA profile (taken in air) of $Ti(SO_4)_2$ impregnated on as-synthesized MCM-41 is shown in Fig. 6 (curve c) in comparison to those of as-synthesized MCM-41 (curve a) and of $Ti(SO_4)_2$ (curve b). Curve (a) shows that most of the surfactant in as-synthesized MCM-41 was decomposed in the temperature range of 200–300 °C. Curve (b) shows that the decomposition of $Ti(SO_4)_2$ is negligible before 300 °C, but around 300–670 °C most of $Ti(SO_4)_2$ decomposed. Curve (c) (the TG profile of $Ti(SO_4)_2$ impregnated on as-synthesized MCM-41) shows several weight loss steps up to 670 °C. Comparing curve c with curve a suggests that the weight loss occurring at temperatures below 300 °C is likely due to the decomposition of surfactant (CTAB). Comparing curve c with curve b suggests that the weight loss occurring at temperatures above 300 °C is attributable to the decomposition of $Ti(SO_4)_2$. In between these two temperatures in curve c there is probably a continuous decomposition of surfactant followed by a gradual decomposition of $Ti(SO_4)_2$. The decomposition of surfactant was apparently slower when $Ti(SO_4)_2$ was present. One possible reason for the slower decomposition is that the interaction between surfactant and sulfate is stronger than that between surfactant and silica. Another is that some small $Ti(SO_4)_2$ crystallites may block the pore mouths of MCM-41 so that the surfactant and/or its decomposition products cannot evaporate as easily as from the pristine MCM-41.

3.5. Catalytic activity of S-TiO_2/MCM-41 in esterification of acetic acid and n-butanol

The esterification of acetic acid and *n*-butanol was carried out using catalyst samples with different TiO_2 loadings. The results

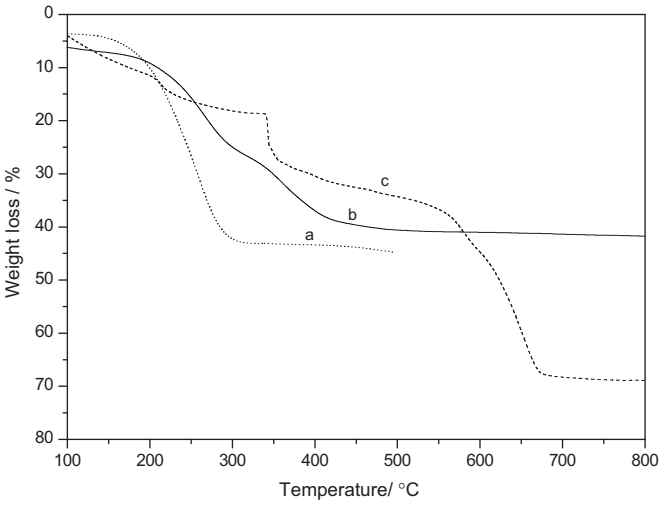

Fig. 6. TGA profiles in air of (a) $Ti(SO_4)_2$, (b) $Ti(SO_4)_2$ impregnated onas-synthesized MCM-41 and (c) as-synthesized MCM-41.

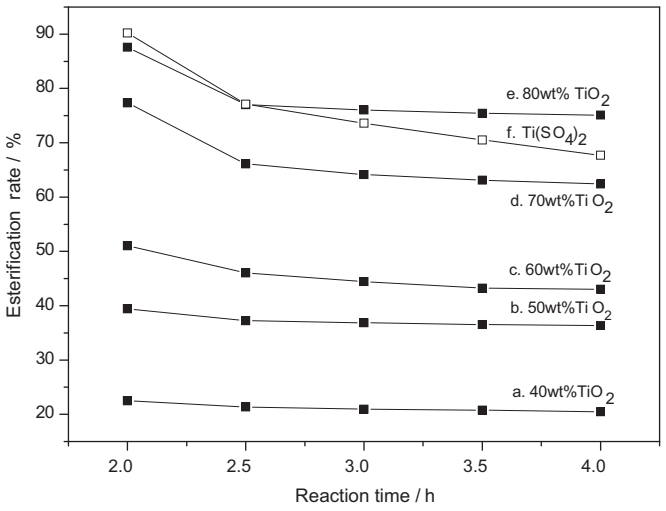

Fig. 7. Esterification rate of acetic acid and *n*-butanol versus time on stream over S-TiO_2/MCM-41 of different TiO_2 loading.

are shown in Table 1 and demonstrate the strong acidity of the S-TiO_2/MCM-41 prepared by direct impregnation method. The results show that the catalytic activity increases with increasing TiO_2 content. The S-TiO_2/MCM-41 catalyst with the highest TiO_2 content (80 wt%) showed similar conversion to the parent $Ti(SO_4)_2$. The same reactions were carried out over a reference catalyst for comparison. The reference catalyst was prepared by impregnating the Ti-sulfate active phase on the MCM-41 substrate after template removal. The amount of sulfur was adjusted to match the concentration of acid sites in S-TiO_2/MCM-41 with 80% TiO_2. The reference catalyst showed a lower conversion compared with S-TiO_2/MCM-41 catalyst with same sulfur content. This indicates the advantage of the proposed method for deposition of Ti-sulfate relative to the traditional method.

Theoretically, the esterification of acetic acid and *n*-butanol is catalyzed by acidic sites. It has been reported that Brönsted acid sites and Lewis acid sites appear on the catalyst surface after the calcination of $Ti(SO_4)_2$. Acid site concentration has been found to have a big effect on the catalytic activity for esterification of acetic acid and *n*-butanol [19]. That is, higher acid site concentration means more catalytically active sites. This will induce higher esterification catalytic activity. From Table 1, it can be seen that the conversion over S-TiO_2/MCM-41 catalysts increased with increasing the sulfur content, i.e. with increasing concentration of the acid sites.

Fig. 7 shows the change in esterification rate with time on stream. All the catalysts showed a similar tendency for the activity to decrease over 4 h from the start of reaction. However, the activity of parent $Ti(SO_4)_2$ decreased rapidly after 2.5 h (Fig. 7). This may be attributable to higher acidity of this catalyst resulting in a large amount of coke being deposited during the reaction.

The high degree of dispersion of this new catalyst has several potential advantages: Its high loading of S-TiO_2 should be favorable for future detailed molecular studies of the catalytic mechanism [20]. Also the effect of promoters should be able to be studied more effectively with these catalysts of larger surface area [21].

4. Conclusions

This paper reports the successful preparation of composites of S-TiO_2/MCM-41 by the direct impregnation method. With this method, S-TiO_2/MCM-41 of high TiO_2 loading can be obtained without destroying the pore structure of MCM-41. The pore size and volume changed significantly with changes in the amount of TiO_2. The catalytic studies on the esterification of acetic acid and *n*-butanol show that the resultants of S-TiO_2/MCM-41 composites have strong acidic properties. The S-TiO_2/MCM-41 catalyst with 80 wt% TiO_2 loading gave the similar activity to the parent $Ti(SO_4)_2$ catalyst after 2 h on stream.

The technique of directly impregnating metal oxide catalyst into the internal surface of mesoporous materials has wide potential applications. The surface reaction of functionalization strongly derived the direct exchange while maintaining the mesostructure. By dispersing the metal containing precursor on the as-synthesized MCM-41 materials the problems of the mesopores completely filling up is avoided. Thereby a supported catalyst of relatively high surface area and with narrowly distributed pore diameter can be prepared.

Acknowledgments

This work was supported by the Key Research Project 06JC14095 of Shanghai Committee of Science and Technology and Shanghai Municipal Natural Science Foundation 07ZR14106.

References

[1] D. Prasetyoko, Z. Ramli, S. Endud, H. Nur, J. Mol. Catal. A: Chem. 241 (2005) 118.
[2] S.M. Jung, O. Dupont, P. Grange, Appl. Catal. A: Gen. 208 (2001) 393.
[3] J.R. Sohn, H.T. Jang, J. Catal. 136 (1992) 267.
[4] A. Mantilla, F. Tzompantzi, G. Ferrat, A. López-Ortega, S. Alfaro, R. Gómez, M. Torres, Catal. Today 107–108 (2005) 707.
[5] Y. Tsutomu, Appl. Catal. 61 (1990) 1.
[6] A.S. Peng, R.J. Ying, X.P. Wang, Speciality Petrochem. 23 (3) (2006) 13.
[7] A. Corma, M.I. Juan-Rajadell, J.M.L. Nieto, Appl. Catal. A 116 (1994) 151.
[8] C.T. Kresge, M.E. Leonowicz, W.J. Roth, J.C. Vartuli, J.S. Back, Nature 359 (1992) 710.
[9] D. Zhao, J. Feng, Q. Huo, N. Melosh, G.H. Fredrickson, B.F. Chmelka, G.D. Stucky, Science 279 (1998) 548.
[10] A. Corma, V. Fornes, M.T. Navarro, J. Perez-Pariente, J. Catal. 148 (1994) 569.
[11] A. Sayari, Chem. Mater. 8 (1996) 1840.
[12] T. Lei, W.M. Hua, Y. Tand, Y.H. Yue, Z. Gao, Chem. J. Chin. Univ. 21 (2000) 1240.
[13] Q.H. Xia, K. Hidajat, S. Kawi, Chem. Commun. (2000) 2229.
[14] C.L. Chen, S. Cheng, H.P. Lin, S.T. Wong, C.Y. Mou, Appl. Catal. A: Gen. 215 (2001) 21.
[15] K.C. Park, D.Y. Yim, S.K. Ihm, Catal. Today 74 (2002) 281.
[16] W.A. Carvalho, P.B. Varaldo, M. Wallau, U. Schuchardt, Zeolites 408 (1997) 18.
[17] C.L. Chen, T. Li, S. Cheng, H.P. Lin, C.J. Bhongale, C.Y. Mou, Micro. Meso. Mater. 50 (2001) 201.
[18] T. Lei, J.S. Xu, Y. Tang, W.M. Hua, Z. Gao, Appl. Catal. A: Gen. 192 (2000) 181.
[19] C.X. Zhang, D.Z. Liao, Z.H. Jiang, Chem 66 (5) (2003) 301.
[20] T.S. Yang, T.H. Chang, C.H. Lin, C.T. Yeh, J. Mol. Catal. A: Chem. 159 (2000) 397.
[21] A. Mantilla, G. Ferrat, A. López-Ortega, E. Romero, F. Tzompantzi, M. Torres, E. Ortíz-Islas, R. Gómez, J. Mol. Catal. A: Chem. 228 (2005) 333.